

Surface Turbulent Flux Measurements over the Loess Plateau for a Semi-Arid Climate Change Study

ZUO Jinqing^{1,2} (左金清), HUANG Jianping¹ (黄建平), WANG Jiemin³ (王介民), ZHANG Wu¹ (张武), BI Jianrong¹ (闭建荣), WANG Guoyin¹ (王国印), LI Weijing² (李维京), and FU Peijian¹ (付培健)

¹College of Atmospheric Sciences, Lanzhou University, Lanzhou 730000

²National Climate Center, China Meteorological Administration, Beijing 100081

³Cold and Arid Regions Environmental and Engineering Research Institute, Chinese Academy of Sciences, Lanzhou 730000

(Received 1 December 2008; revised 2 January 2009)

ABSTRACT

In order to provide high quality data for climate change studies, the data quality of turbulent flux measurements at the station of SACOL (Semi-Arid Climate & Environment Observatory of Lanzhou University), which is located on a semi-arid grassland over the Loess Plateau in China, has been analyzed in detail. The effects of different procedures of the flux corrections on CO₂, momentum, and latent and sensible heat fluxes were assessed. The result showed that coordinate rotation has a great influence on the momentum flux but little on scalar fluxes. For coordinate rotation using the planar fit method, different regression planes should be determined for different wind direction sectors due to the heterogeneous nature of the ground surface. Sonic temperature correction decreased the sensible heat flux by about 9%, while WPL correction (correction for density fluctuations) increased the latent heat flux by about 10%. WPL correction is also particularly important for CO₂ fluxes. Other procedures of flux corrections, such as the time delay correction and frequency response correction, do not significantly influence the turbulent fluxes. Furthermore, quality tests on stationarity and turbulence development conditions were discussed. Parameterizations of integral turbulent characteristics (ITC) were tested and a specific parameterization scheme was provided for SACOL. The ITC test on turbulence development conditions was suggested to be applied only for the vertical velocity. The combined results of the quality tests showed that about 62%–65% of the total data were of high quality for the latent heat flux and CO₂ flux, and as much as about 76% for the sensible heat flux. For the momentum flux, however, only about 35% of the data were of high quality.

Key words: eddy covariance, turbulent fluxes, flux corrections, quality control, SACOL

Citation: Zuo, J. Q., J. P. Huang, J. M. Wang, W. Zhang, J. R. Bi, G. Y. Wang, W. J. Li, and P. J. Fu, 2009: Surface turbulent flux measurements over the Loess Plateau for a semi-arid climate change study. *Adv. Atmos. Sci.*, **26**(4), 679–691, doi: 10.1007/s00376-009-8188-2.

1. Introduction

As the problems of global warming and extreme weather and climate events become more serious, climate change has been the focus of experimental researches and numerical simulations for the past decades and continues to be one of the central research topics in the world. The study of land surface processes (LSP), which control the exchanges of energy and mass fluxes between the surface and the

atmosphere, is one of the most basic aspects of climate change research. As one of the processes of LSP, exchanges of energy and mass fluxes between the surface and the atmosphere have been of more concern in China (Zhu et al., 2003; Liu et al., 2004; Lü et al., 2005; Yu et al., 2006; Huang et al., 2008). These measurements can provide important data not only for the researches of a regional response to global climate change but also validation of the parameterization scheme of LSP in climate models. At the same

Corresponding author: HUANG Jianping, hjp@lzu.edu.cn

time, the eddy covariance (EC) technique provides a powerful tool for the direct measurement of energy and mass fluxes between the surface and the atmosphere (Foken and Wichura, 1996; Aubinet et al., 2000; Lee et al., 2004). Moreover, fast-response anemometers, gas analyzers, and data acquisition and processing systems are becoming more reliable, affordable, and easier to use. As a consequence, the EC method has been widely used for turbulent flux measurements. As of 30 March 2008, there have been 543 sites registered on the FLUXNET, a global network of micrometeorological tower sites that use EC methods to measure the exchanges of CO₂, water vapor, and energy between the terrestrial ecosystem and the atmosphere (<http://www-eosdis.ornl.gov/FLUXNET/>). This network includes several regional flux networks such as AmeriFlux, AsiaFlux, CarboEurope IP, ChinaFLUX, KoFlux, Fluxnet-Canada, and OzFlux, and it covers various ecosystems including forests, crops, grasslands, chaparral, wetlands, and tundra (Baldocchi et al., 2001). There are also tens of flux stations coordinated by CEOP (Coordinated Enhanced Observing Period) (www.ceop.net).

Though the EC method is considered as a standard method for the direct measurement of turbulent fluxes, it has been subjected to a set of problems, such as the surface energy balance closure (Culf et al., 2004; Oncley et al., 2007), underestimation of nighttime CO₂ flux (Goulden et al., 1996), and intermittency under stably stratified atmospheric conditions. For this method in its simplified form, there are several basic theoretical assumptions, i.e., the stationarity of the flow, homogeneity of the underlying surface, fully developed turbulence, and existence of a constant flux layer, etc. (Foken and Wichura, 1996). These assumptions, however, can not be fulfilled especially under complicated conditions, such as rolling terrain, patchy vegetation, and unfavorable meteorological conditions. Studies have shown that these complicated conditions have critical impacts on EC measurements (Gao et al., 2006; Wang et al., 2007). Therefore, quality assurance and quality control (QA/QC) are essential for turbulent flux measurements. Moreover, studies *in situ* are required as real situations are specific for each site, especially for sites on complicated terrain.

Many studies have focused on the QA/QC of EC measurements. Major algorithms for flux corrections applied during post-field data processing are now available, such as coordinate rotation (Kaimal and Finnigan, 1994; Wilczak et al., 2001), frequency response corrections (Moore, 1986; Horst, 1997; Goulden et al., 1997; Massman, 2000), sonic temperature correction (Schotanus et al., 1983; Liu et al., 2001), and density effect correction (Webb et al., 1980). Furthermore,

quality tests on flux sampling problems, stationarity, and turbulence development conditions, which are important to identify inferior data, have also been widely studied (Foken and Wichura, 1996; Goulden et al., 1996; Foken et al., 2004; Gu et al., 2005; Loescher et al., 2006).

The quality control, however, contains some very site-specific tests (Foken et al., 2004). Moreover, unlike the situation of a flat homogeneous terrain, turbulent flux measurements over heterogeneous terrain or limited fetch is still being studied. Therefore, this paper attempts to explore the impacts of various procedures of flux corrections, especially the coordinate rotation by the planar fit method, on turbulent flux measurements over a semi-arid grassland on the Loess Plateau in China. This study will also focus on quality tests on flux sampling problems, stationarity, and in particular on turbulence development conditions.

2. Experimental set-up

The station SACOL, established in 2006, is a long-term meteorological observatory operated by the College of Atmospheric Sciences, Lanzhou University. It is located at (35° 57' N, 104° 08' E) with an elevation of 1965.8 m, about 48 km away from the centre of Lanzhou, Gansu Province in northwestern China. The station is situated at the southern bank of the Yellow River, a semi-arid area on the Loess Plateau in China. The soil parent material is mainly quaternary aeolian loess with the soil type of Sierozem according to the Chinese Soil Classification System (Chinese Soil Taxonomy Cooperative Research Group, 1995). Figure 1

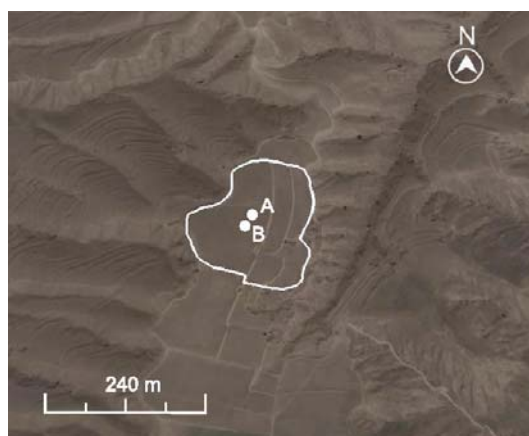


Fig. 1. The topographic features of the SACOL site from the latest version of Google Earth (Version: 4.3.7284.3916, Build Date: 8 Jul 2008). A: 32-m tower for routine boundary-layer meteorological measurements and B: a 3-m tower for eddy covariance measurements.

shows the topographic features of this site. The surface is mainly covered by short grass with species of *stipa bungeana*, *artemisia frigida*, and *leymus secalinu*. The site is located on a nearly north-south mesa with a fetch length of about 120 m in the most common wind direction. The mesa has a limited width of about 200 m from the east to the west, and is about 600 m in length from the north to the south. There is a large V shape valley to the west of the site and a small one to the east. More details relating to the site and instrumentation can be found in a report by Huang et al. (2008).

The turbulent flux measurement system consists of a three-axis sonic anemometer (CSAT3, Campbell) to measure three wind components and sonic virtual temperature, and an open path infrared CO₂/H₂O analyzer (LI7500, LI-COR) to measure CO₂ and H₂O concentrations. The observations were taken at 3.0 m above the ground surface with signals acquired by a CR5000 (Campbell) data logger at 10 Hz. A slow response humidity and temperature probe (HMP45C-L, Vaisala) was also set near and at the same level of the open-path eddy covariance flux system. Supporting data include measurements of the surface skin temperature (IRTS-P, Apogee), soil temperature at depths of 2, 5, 10, 20, 50, and 80 cm (STP01-L, Hukseflux), and soil water content at depths of 5, 10, 20, 40, and 80 cm (CS616-L, Campbell). The soil heat flux was measured with a self-calibrating soil heat flux plate (HFP01SC-L, Hukseflux) at depths of 2 and 5 cm. In addition, the incoming and outgoing shortwave radiation fluxes were measured with a pyranometer (CM21, Kipp & Zonen), and the incoming and outgoing long-wave radiation fluxes with a pyrgeometer (CG4, Kipp & Zonen) at a height of 1.5 m.

3. Analysis methods

3.1 Eddy covariance method

The eddy covariance (EC) method (Swinbank, 1951) is the basis of the turbulent flux measurements and will be briefly described in this section. The vertical flux F of a scalar S is defined as:

$$F = \frac{1}{T} \int_0^T w s dt, \quad (1)$$

where w and s are the fluctuations of the vertical velocity and the concentration of S , respectively; and T is the averaging period. Using the Reynolds decomposition ($w = \bar{w} + w'$, $s = \bar{s} + s'$, where $\bar{}$ denotes the expected value and \prime the fluctuation), the flux can be rewritten in the form:

$$F = \bar{w}\bar{s} + \overline{w's'}, \quad (2)$$

where the first term of the right hand side of Eq. (2) represents the vertical advection; and the second term denotes the turbulent flux. With the assumption that $\bar{w} = 0$, the fluxes of sensible heat (H), latent heat ($L_v E$, where L_v is the latent heat for vaporization, and E is the water vapor flux), carbon dioxide (F_c), and momentum (τ) are given by Eqs. (3) to (6), respectively:

$$H = \rho c_p \overline{w T_s}, \quad (3)$$

$$L_v E = L_v \overline{w \rho_v}, \quad (4)$$

$$F_c = \overline{w \rho_c}, \quad (5)$$

$$\tau = -\rho u^2, \quad (6)$$

where the friction velocity,

$$u = (\overline{u^2} + \overline{v^2})^{1/4}. \quad (7)$$

And the stability parameter is defined as:

$$\zeta = \frac{z}{L} = -\frac{(z_m - d)\kappa(g/\bar{T})\overline{w T}}{u^3}, \quad (8)$$

where ρ (kg m⁻³) is the air density; ρ_v and ρ_c (kg m⁻³) are the concentration fluctuations of water vapor and CO₂, respectively; w , u and v (m s⁻¹) are the fluctuations of the wind velocities; T_s (K) is the fluctuation of the sonic temperature; c_p [$c_p = 1004.67(1 + 0.84q)$, J K⁻¹ kg⁻¹] is the specific heat of air; q is the specific humidity; L_v ($L_v = 2.5008 - 0.0023668T_s$, J kg⁻¹; List, 1951) is the latent heat for the vaporization of water; T_s (°C) is the sonic temperature; z_m (m) is the measurement height; d (m) is the zero plane displacement and set to be zero as the grass was very short and sparse; g (m s⁻²) is the acceleration due to gravity; L is the Monin-Obukhov length, and κ ($=0.4$) is the von Karman constant.

3.2 Stationarity test

Stationary means that the turbulent statistics (e.g., averages and variances) do not change in time (Panofsky and Dutton, 1984; Foken et al., 2004). Non-stationarity in the time series often occurs with mesoscale or synoptic-scale variability, or changes of internal boundary layers or the footprint over an inhomogeneous surface (Vickers and Mahrt, 1997; Foken et al., 2004). The procedure designed for the stationarity test used in this study was proposed by Foken and Wichura (1996). The test compares the covariance of the averaging period with the arithmetic mean of the covariances of short intervals within this period, and agreement between both values is a measure of steady state conditions.

The measured time series of about a 30-minute duration will be divided into $M = 6$ intervals of 5 minutes each. The covariance of the measured signals w (e.g.,

vertical velocity) and x (e.g., CO₂ concentration) of the single short interval is defined as

$$(\overline{xw})_i = \frac{1}{N-1} \left(\sum_{j=1}^N x_j w_j - \frac{1}{N} \sum_{j=1}^N x_j \sum_{j=1}^N w_j \right), \quad (9)$$

where N is the measuring points of the short interval.

The mean covariance of the M short intervals is given by

$$(\overline{xw})_s = \frac{1}{M} \sum_{i=1}^M (\overline{xw})_i. \quad (10)$$

The covariance of the whole interval is defined as

$$(\overline{xw})_w = \frac{1}{MN-1} \left(\sum_{j=1}^{MN-1} x_j w_j - \frac{1}{MN} \sum_{j=1}^{MN} x_j \sum_{j=1}^{MN} w_j \right). \quad (11)$$

The difference (P_{SS}) between both covariances, a measure of steady state conditions, is defined as

$$P_{SS} = \left| \frac{(\overline{xw})_s - (\overline{xw})_w}{(\overline{xw})_w} \right|. \quad (12)$$

If the parameter P_{SS} is less than 30%, the time series is considered to be stationary.

3.3 Integral turbulence characteristics test

Assumptions in the eddy covariance technique require turbulence development conditions, i.e., shear stress and surface heating, and sometimes these conditions are weak or absent, especially during nocturnal periods. Researchers have found that the integral turbulence characteristics (flux-variance similarity), which are basic similarity characteristics of the atmospheric turbulence, are good measures describing atmospheric turbulent conditions in the surface layer (Foken and Wichura, 1996; Foken et al., 2004; Mauder and Foken, 2004). According to Foken et al. (2004), the integral turbulent characteristics of wind components are given by

$$\frac{\sigma_{u,v,w}}{u} = c_1 \left(\frac{z}{L} \right)^{c_2}, \quad (13)$$

and the integral turbulent characteristic of temperature is given by

$$\frac{\sigma_T}{T} = c_3 \left(\frac{z}{L} \right)^{c_4}, \quad (14)$$

where T is the temperature scale, and $c_1, c_2, c_3,$ and c_4 are constants, which are determined by experiments.

The difference (P_{ITC}) between the measured and modeled parameters according to Eq. (13) or Eq. (14) is a measure of turbulence development conditions, and defined as

$$P_{ITC} = \left| \frac{(\sigma_x/X)_{mo} - (\sigma_x/X)_{ms}}{(\sigma_x/X)_{mo}} \right|, \quad (15)$$

where the subscript ms and mo denote the measured parameter and the modeled parameter according to Eq. (13) or Eq. (14), respectively. If the test parameter P_{ITC} is less than 30%, the turbulence can be considered as a well developed turbulence. The integral turbulent characteristics test (ITC test) is not applied for the sensible heat flux under neutral conditions since the integral turbulence characteristics of the scalars have extremely high values (Foken and Wichura, 1996; Foken et al., 2004).

4. Results and discussion

4.1 Flux calculation and corrections

The data collected during 13–31 May 2006, were selected and analyzed in detail. These days were relatively sunny except when a short and weak rain event occurred on 19, 20, and 25 May. An averaging period of 30 minutes was used in this study. In order to reduce the flow distortion by the instrument frame, only the data collected over a range of wind directions from -90° to 90° in the sonic anemometer coordinate system were selected for this study.

4.1.1 Basic test of the raw data

The first step for data processing for the eddy covariance measurements is the basic test of raw data. Each time series was tested for physical plausibility by simply comparing the minimum and maximum values of all the points in the record to certain fixed limits that were considered unphysical. For this study, the absolute limits are 30 m s^{-1} for the horizontal wind components, 5 m s^{-1} for the vertical wind, -50 C to 60 C for the sonic temperature, 200 mg m^{-3} to 1000 mg m^{-3} for the CO₂ concentration, 0 g m^{-3} to 30 g m^{-3} for the water vapor density, and 50 kPa to 120 kPa for the air pressure.

Furthermore, each time series was screened using the algorithm from Vickers and Mahrt (1997) to detect the remaining spikes in the high-frequency time series and the discarded values were interpolated. Any point that is more than 4.0 times the standard deviation from the mean in a window of 60 seconds is considered a spike. When the total number of spikes and the points with unrealistic data values exceed 1% of the total number of data points, the entire data run is discarded from further study. The incomplete records,

with a threshold of 5 minutes, are also removed. The results show that the spikes do not significantly influence the turbulent flux measurements.

Then, variances and covariances were obtained by block averaging (i.e., mean removal) of 30 minutes. A potential time delay due to the longitudinal sensor separation between the sonic anemometer and the gas analyzer is considered by cross-correlation analysis (time delay correction) for each averaging interval. The bounds of lag-time are set to be 1.0 s (Vickers and Mahrt, 1997; Berger et al., 2001).

Unusually small or large statistics such skewness, kurtosis, and variance often indicate an instrument problem (Foken et al., 2004). If the statistic is smaller or larger than a fixed limit, the whole record is considered subject to instrument problems and will be discarded. In this study, this problem was detected by comparing the variance to prescribed thresholds, which is determined empirically from examining frequency distributions of the parameter itself. The thresholds are $3 \text{ m}^2 \text{ s}^{-2}$ for the horizontal wind component, $1.5 \text{ m}^2 \text{ s}^{-2}$ for the vertical wind component, $10 \text{ mg}^2 \text{ m}^{-6}$ for the CO_2 concentration, $4 \text{ g}^2 \text{ m}^{-6}$ for the water vapor density, and $2 (\text{C})^2$ for the sonic temperature. There were about 4% of the total data runs that were detected and removed for a 19-day period in May 2006.

4.1.2 Coordinate rotation

A coordinate rotation should be performed on the wind data to eliminate the effects of instrument tilt as well as terrain irregularity on the airflow from the fluxes by placing the sonic anemometer into a streamline coordinate system. The common rotation algorithms include double rotation (DR) (Kaimal and Finnigan, 1994) and planar fit (PF) (Wilczak et al., 2001). There is also a triple rotation (TR) method, which is similar to the DR method but requires a triple rotation of the anemometer axes to set the lateral momentum flux equal to zero. The TR method, however, is shown to result in great stress errors due to errors in the measured mean velocities and stresses, in particular the cross-wind stress (Wilczak et al., 2001). So only the DR and PF methods are compared with each other, and the PF method is preferred in this study (Wilczak et al., 2001; Moene et al., 2002; Foken et al., 2004). For the PF method, the tilt angles in the x - z and y - z planes are 1.2° and 0.5° , respectively for all the wind directions (Table 1). The tilt error in the sum of the sensible and latent heat fluxes ($H + L_v E$) is small (about 1.5%), while it is significant in the momentum flux. The corrected momentum flux is approximately 5% larger than the uncorrected flux, which is in agreement with Wilczak et al. (2001) who showed that the

errors for and were approximately 6% per degree of tilt in the x - z and y - z planes. In addition, the difference of tilt errors between the PF and DR algorithms is small for the scalar fluxes, while the difference is about 11% for the momentum flux.

Due to the heterogeneity of the underlying surface of the measuring site, the flow patterns may be different between different wind directions. As showed in Fig. 2, the wind commonly comes from the SE and NW directions. The geographic conditions, however, are significantly different between these two wind directions, which may imply an influence on the tilt errors. Therefore, the wind data were separated into two different sectors to determine two different regression planes. The first sector is called the SE sector from 60° to 240° , and the remaining sector is the NW sector from 240° (through 360°) to 60° . Then, the two planes were fitted by multiple linear regression analyses. As shown in Table 1, the tilt angles in the SE sector are different from those in the NW sector. To avoid confusion, here we use scheme 1 to denote the PF-correction with one fitted plane for all the data from all wind directions, and scheme 2 to denote the PF-correction with two fitted planes for two different wind sectors. The results show that the PF-corrected momentum flux using scheme 1 is about 7% larger than that using scheme 2, while the effect of scheme 1 to the sensible and latent heat fluxes is small compared to scheme 2. This indicated that the PF-correction, which considers different fitted planes for different wind sectors, is particularly important for the momentum flux. Therefore, we recommend that different regression planes should be determined for different wind direction sectors due to the heterogeneities of the measuring site.

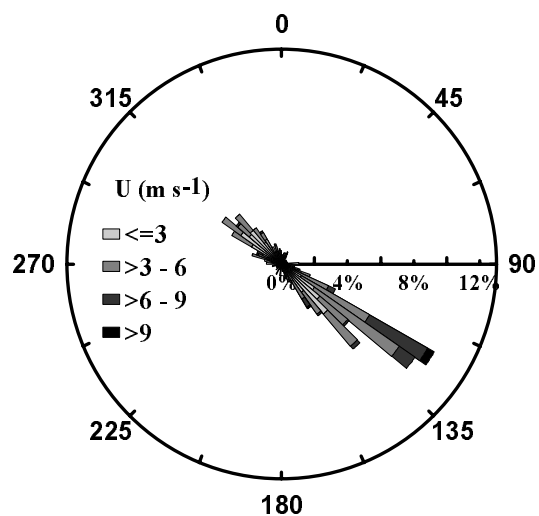


Fig. 2. Frequency distribution of the wind direction and wind speed (U) during 13–31 May 2006.

Table 1. Tilt angles in the x - z and y - z planes detected by the planar fit method.

Range of wind directions	Tilt angle in the x - z plane	Tilt angle in the y - z plane
0 -360	1.2	0.5
60 -240	1.5	1.1
240 -60	0.3	0.6

4.1.3 Frequency response corrections

All eddy covariance systems display some frequency attenuations at sufficiently high and low frequencies (e.g., Moore, 1986). These attenuations mainly result from the frequency dynamical response, sensor separation, path-length averaging effects associated with the sensor design, frequency response mismatch, high pass filtering, low pass filtering, and digital sampling (Moore, 1986; Horst, 1997; Goulden et al., 1997; Massman, 2000, 2001; Rannik, 2001; Massman and Lee, 2002; Burba and Anderson, 2007). There are several different methods to compensate for the flux losses due to frequency attenuations at different frequencies of turbulent transport, such as Moore's approach (Moore, 1986), the low-pass filtering method (Goulden et al., 1997), and the analytical method developed by Massman (2000), which was incorporated and extended from Horst's approach (1997). The analytical method is preferred in this study as it is a relatively comprehensive numerical approach, which includes corrections not only for high frequency attenuations but also for low frequency attenuations.

According to Massman (2000), the analytical formula for the frequency response corrections to measured momentum and scalar fluxes with fast-response open path systems is

$$\frac{F_m}{F} = \left[\frac{a^\alpha b^\alpha}{(a^\alpha + 1)(b^\alpha + 1)} \right] \left[\frac{a^\alpha b^\alpha}{(a^\alpha + p^\alpha)(b^\alpha + p^\alpha)} \right] \times \left[\frac{1}{(p^\alpha + 1)} \right] \left[1 - \frac{p^\alpha}{(a^\alpha + 1)(a^\alpha + p^\alpha)} \right], \quad (16)$$

where F_m denotes the measured flux and F the true eddy flux; and $\alpha = 0.925$ for $z/L \leq 0$ and $\alpha = 1$ for $z/L > 0$. Here $a = 2\pi f_x \tau_h$, $b = 2\pi f_x \tau_b$, and $p = 2\pi f_x \tau_e$, where τ_h is the equivalent time constants associated with trend removal, τ_b is the equivalent time constants associated with block averaging and mean removal, and τ_e is the equivalent first order time constant for the entire set of low pass filters associated with path-length averaging, sensor separation, finite response times, etc. [see Table 1 and Eq. (9) of Massman, 2000]. f_x is the frequency of the peak of the logarithmic cospectrum and can be estimated from $f_x = n_x u / z$, where z denotes the measurement height, u the mean horizontal wind speed at that height, and n_x is the non-dimensional frequency corresponding to

f_x . Generally, n_x is parameterized as a function of stability. In this study, f_x is determined using cospectral models adapted from Kaimal et al. (1972) by Kaimal and Finnigan (1994), i.e., $n_x = 0.079$ for $z/L \leq 0$, and $n_x = 0.079(1 + 7.9z/L)^{3/4}$ for $z/L > 0$.

For the open path system in this study, the lateral separation is 0.2 m, and no longitudinal separation is assumed. No anti-noise filter or recursive digital filter is applied to the measured signals. The sonic anemometer has collocated horizontal and vertical paths of length 0.12 m, and the gas analyzer has a sensor path of length 0.125 m. The frequency response corrections applied to the measured fluxes in this study include vector/scalar line averaging, sensor lateral separation, blocking averaging, and mean removal. The results show the effects of these corrections on the momentum flux and on the scalar fluxes are small (less than 1%), which indicate that the flux losses due to high and low frequency attenuations are small for the CO_2 flux, momentum flux, and latent and sensible heat fluxes.

4.1.4 Sonic temperature correction

The sonic temperature T_s measured by a sonic anemometer is derived from the sonic velocity, which depends on both the air temperature and humidity. The fluctuations of sonic temperature includes the effect of humidity on the speed of sound (c), and should be converted into actual temperature (Schotanus et al., 1983),

$$T_s = T(1 + 0.51q). \quad (17)$$

And the corrected sensible heat flux is calculated after

$$\overline{wT} = \overline{wT_s} - 0.51\overline{T} \overline{wq} + 2 \frac{\overline{T} \overline{uw} u}{c^2}. \quad (18)$$

On average, for all stabilities, this correction reduces the sensible heat flux by about 9%, while the change in temperature is not significant (less than 0.5%). Researchers (Schotanus et al., 1983; Liu et al., 2001) have found that the changes resulting in a sonic temperature correction were different between stable and unstable stratifications. Liu et al. (2001) reported that the corrected sensible heat flux \overline{wT} is around 10% lower than the sonic derived buoyancy flux $\overline{wT_s}$ in stable stratification, and \overline{wT} is as much as 30% lower than $\overline{wT_s}$ in unstable stratification. In

this study, \overline{wT} is about 4% lower than $\overline{wT_s}$ in stable stratification, and \overline{wT} is about 12% lower than $\overline{wT_s}$ in unstable stratification.

4.1.5 WPL correction

It is widely accepted that the WPL correction proposed by Webb et al. (1980) is required for the determination of the density effects due to heat and water vapor transfer on turbulent flux measurements. This correction for the CO₂ flux is particularly significant because the vertical advection term ($\overline{\rho_c w}$) and the turbulent flux ($\overline{\rho_c w}$) of ten have similar magnitudes (Leuning et al., 1982). The corrected latent heat flux is given by

$$L_v E = L_v (1 + \mu\sigma) \{ \overline{w \rho_v} + (\overline{\rho_v / T}) \overline{w T} \}. \quad (19)$$

And the corrected CO₂ flux is in terms of the sensible heat flux and the WPL-corrected latent heat flux, and given by

$$F_c = \overline{w \rho_c} + \mu (\overline{\rho_c / \rho_a}) \overline{w \rho_v} + (1 + \mu\sigma) (\overline{\rho_c / T}) \overline{w T}, \quad (20)$$

where $\sigma = \overline{\rho_v} / \overline{\rho_a}$, is the ratio of the mean densities of water vapor and dry air; $\mu = m_a / m n_v = 1.6$, the ratio of the molecular masses of dry air and water vapor; $\overline{\rho_c}$, the mean density of CO₂ concentration; and \overline{T} , the mean absolute temperature at the measurement height.

Figure 3a shows daily variations of the CO₂ flux before and after the WPL correction. For a better visualization, only 4 days (14–18 May 2006) were shown here. There is a significant but illusive daily change that arises from the presence of heat and water vapor fluxes. The corrected upward and downward CO₂ fluxes, which represent the actual exchange of CO₂ between the surface and the atmosphere, are approximately zero in this period. Further analysis shows that the WPL-corrected CO₂ fluxes are also very small in the following summer. The weak CO₂ exchange is mainly attributed to the short and sparse vegetation, and in particular the extreme drought this year. The grass growth over this area was limited by the dryness of the soil. Figure 3b shows daily variations of the latent heat flux before and after the WPL correction. The result shows that the WPL correction to the latent heat flux results in a significant increase during the daytime, while a small change during the nighttime. This correction enlarges the latent heat flux by about 10%.

4.2 Quality control

A quality classification scheme (Table 2) proposed by Foken et al. (2004) is used to classify the stationarity test into different quality levels according to

